

Published in final edited form as:

Arch Oral Biol. 2015 January ; 60(1): 1–11. doi:10.1016/j.archoralbio.2014.08.022.

Temporomandibular Joint Fibrocartilage Degeneration from Unilateral Dental Splints

Sarah E. Henderson, B.S.¹, Jesse R. Lowe, M.S.¹, Mauro A. Tudares, M.S.², Michael S. Gold, Ph.D.³, and Alejandro J. Almarza, Ph.D.^{1,2,4,*}

¹Department of Bioengineering, University of Pittsburgh, Pittsburgh, PA

²Department of Oral Biology, University of Pittsburgh, Pittsburgh, PA

³Department of Anesthesiology, University of Pittsburgh, Pittsburgh, PA

⁴McGowan Institute for Regenerative Medicine, University of Pittsburgh, Pittsburgh, PA

Abstract

Objective—The objective of this study was to determine the extent to which altered loading in the temporomandibular joint (TMJ), as might be associated with a malocclusion, drives degeneration of articulating surfaces in the TMJ. We therefore sought to quantify the effects of altered joint loading on the mechanical properties and biochemical content and distribution of TMJ fibrocartilage in the rabbit.

Design—Altered TMJ loading was induced with a 1 mm splint placed unilaterally over the maxillary and mandibular molars for six weeks. At that time, TMJ fibrocartilage was assessed by compression testing, biochemical content (collagen, glycosaminoglycan (GAG), DNA) and distribution (histology), for both the TMJ disc and the condylar fibrocartilage.

Results—There were no changes in the TMJ disc for any of the parameters tested. The condylar fibrocartilage from the splinted animals was significantly stiffer and the DNA content was significantly lower than that in control animals. There was significant remodeling in the condylar fibrocartilage layers as manifested by a change in GAG and collagen II distribution and a loss of defined cell layers.

Conclusions—A connection between the compressive properties of TMJ condylar fibrocartilage after 6 weeks of splinting and the changes in histology was observed. These results suggest a change in joint loading, leads to condylar damage, which may contribute to pain associated with at least some forms of TMJ disease.

© 2014 Elsevier Ltd. All rights reserved.

*Corresponding Author: Department of Bioengineering, University of Pittsburgh, 566 Salk Hall, 3501 Terrace Street, Pittsburgh, PA, 15261, USA, Telephone: 412-648-8500, Fax: 412-624-6685, aja19@pitt.edu.

Conflict of Interest Statement: The authors have no conflicts of interest to disclose.

Publisher's Disclaimer: This is a PDF file of an unedited manuscript that has been accepted for publication. As a service to our customers we are providing this early version of the manuscript. The manuscript will undergo copyediting, typesetting, and review of the resulting proof before it is published in its final citable form. Please note that during the production process errors may be discovered which could affect the content, and all legal disclaimers that apply to the journal pertain.

Keywords

temporomandibular joint; fibrocartilage degeneration; unilateral dental splint

Introduction

The development of effective interventions for the treatment of temporomandibular joint (TMJ) disorders (TMD) has been hindered by the fact that preclinical models of TMD inadequately reflect the pathology of the human state. Patients who undergo surgery often have both pain and abnormal joint functional loading (1, 2). In more severe cases, there is also degeneration of the articulating tissues, including the TMJ disc and the condylar fibrocartilage (3). However, it is not clear whether abnormal loading leads to degeneration and then pain, or degeneration leads to abnormal loading and pain. In support of the latter, trauma, internal derangement, and parafunctional habits are all thought to be able to initiate the cascade of events that lead to TMD (3, 4). The link between parafunctional habits and TMD would also support the suggestion that altered loading is the cause rather than the effect in the case of TMD where, in the case of bruxism (clenching), joint overloading would lead to biochemical changes in the synovial fluid and painful inflammation, which then causes adhesions and immobilization of the joint, leading to further alterations to the articulating surfaces (1). In severe cases, the alteration could be a pathological process of joint degeneration, such as osteoarthritis, which is characterized by deterioration and abrasion of the articulating fibrocartilage and local thickening and remodeling of the underlying bone (5).

Unfortunately, despite the development of several different preclinical models designed to drive TMD by changes in joint loading (6-19), there have been no detailed analyses of the articulating surfaces in the TMJ. Rather, changes to the articulating surfaces have only been suggested with results of histological analysis where differences in the distribution of extracellular matrix components in the condyle have been described (13, 14). However, the mechanical properties and quantitative biochemical properties of the fibrocartilage are lacking, which can give more insight into the degeneration process.

Therefore, the objective of this study was to determine the effects of altered TMJ loading on the properties of TMJ fibrocartilage. TMJ fibrocartilage was assessed mechanically in compression and the biochemical content and distribution were determined. The hypothesis was that altered mechanical and biochemical properties and disorganized cellular presence in histology would serve as indicators for the presence of remodeling.

Materials and Methods

Animal Model

The majority of previous TMD animal studies have been completed on small rodents (20). However, these small rodent animal models do not lend themselves to mechanical analysis of the articulating joint tissue, while the TMJ's main function is mechanical support of jaw movement. Consequently, the rabbit model was used in the present study, taking advantage

of the facts that there is sufficient articulating joint tissue for mechanical analysis and TMJ injury and degeneration models already established in the literature (13, 18, 20-26). A unilateral molar splint (13, 17, 18), was chosen for this study because it is associated with altered TMJ loading, in the absence of a direct manipulation of the joint, and most closely mirrors changes driven by a sudden change in malocclusion occurring from trauma or a radical dental procedure.

Skeletally mature, female, New Zealand White rabbits approximately 1 year in age and weighing between 5-7 kg were purchased from Myrtle's Rabbitry Inc. (Thompsons Station, TN), and Charles River Laboratories International, Inc. (Wilmington, MA). All rabbits were examined by a veterinarian prior to use in the study and were found to be in good health. All animal procedures were approved by the Institutional Animal Care and Use Committee at the University of Pittsburgh and in accordance with the National Institutes of Health guidelines for the use of laboratory animals.

All of the experimental group (splinted) rabbits were sedated with intramuscular ketamine (20 mg/kg) and xylazine (2 mg/kg) and maintained in a surgical plane of anesthesia with inhaled 2% isoflurane for two separate procedures: impressions and splint placement. During the first procedure, impressions were taken of the upper and lower right molars (Figure 1A). Non-precious metal bite-raising splints were cast as crowns on molds made from the impressions (Figure 1B). The thickness of each splint was approximately 1 mm. During the second procedure, the right molars were cleaned (with water and a cotton swab to remove food debris) and primed (with 34% Phosphoric Acid Tooth Conditioner Gel, Dentsply International Inc, Milford, DE), and the splints were attached with dental cement (GC FujiCEM 2, GC Corporation, Tokyo Japan) (Figure 1C). Splint placement was verified after 1 week of placement. There were some animals (approximately 50%) where the upper splint fell off the molars after one to two weeks, but in all cases the lower splint remained in place throughout the experimental period. There were no statistical differences between the rabbits with one versus two splints in place at the end of the experimental period.

After 6 weeks, the rabbits were euthanized (100 mg/kg pentobarbital) and the TMJ tissues were harvested and processed for histology or were stored by wrapping in phosphate buffered saline (PBS) soaked gauze and freezing at -20 °C until future use for biomechanical and biochemical testing. The samples were stored at -20 °C for at least several months. Prior to freezing the samples were wrapped in PBS soaked gauze. Before mechanical testing the samples were thawed and allowed to rehydrate in room temperature PBS for at least an hour. Freeze thaw cycles have been previously shown not to affect mechanical properties up to 5 freeze thaw cycles (27). The length of time frozen could have affected the results, however, the samples from the respective groups were all frozen a similar amount of time and went through a similar number of freeze thaw cycles, so would be affected in a similar manner.

Unconfined Compression Testing – TMJ Disc

To characterize the compressive properties of the TMJ disc (n=8 per group), stress relaxation testing in unconfined compression was completed using an MTS Insight (Eden Prairie, MN) on cylindrical plugs (diameter = 2 mm) (28) (Figure 2A, B). Samples were taken from the medial side of the intermediate zone of the discs, from both left and right

discs of control and splinted animals. The samples were placed in a PBS water bath at a physiological temperature of 37 °C. First, the samples were exposed to a preload of 0.05 N to ensure contact with the surface, and determine the initial height of the sample. Ten cycles of preconditioning at a constant strain rate of 9% per minute to 10% strain was completed. Samples were then tested in stress relaxation to 10% strain and allowed to relax for 30 minutes (28-30). The samples were then compressed in 5% increments to 30% strain, with 30 minutes of relaxation in between steps (Figure 2C). The force and distance traveled were recorded throughout the test and were normalized to stress and strain, respectively. The peak stress was determined for each strain level, as well as the change in stress after the relaxation period resulting in the percent relaxation. The tangent modulus was calculated by finding the slope of the last 20% of the linear region of the loading curve for each strain step (Figure 2D). A two-way ANOVA with Tukey's post hoc test ($p < 0.05$) was used to determine if there were any significant differences between the variables at each strain step based on sample side (left/right) and experimental treatment (control/splinted).

Compression Testing to a Certain Force - Condylar Fibrocartilage

Compression testing to a certain force was used to test the condylar fibrocartilage because the fibrocartilage was too thin to remove from the bone consistently which was required for unconfined compression testing. The left and right condyles of splinted and control rabbits were tested in two regions: an anterior region and a posterior region ($n=8$). An indenter (Figure 3A), 1 mm in diameter, was compressed into the fibrocartilage on bone at a constant rate of 0.1 mm/min until a force of 0.02 N (25.4 kPa) was reached, recording the force and the distance traveled (Figure 3B). The thickness of the fibrocartilage was measured using a needle technique (31), in which a needle was inserted through the fibrocartilage and bone at a constant rate of 0.1 mm/min until a force of 0.2 N was reached (Figure 3C), indicating full travel through the fibrocartilage and into the bone. The thickness of the fibrocartilage was determined to be the displacement when the slope of the loading curve was equal to 1 N/mm. The strain at 0.02 N was calculated by dividing the distance traveled by the indenter to 0.02 N by the thickness determined from the needle test. A two-way ANOVA was completed with Tukey's post hoc test ($p < 0.05$) to determine by region if there were differences between left and right condyles and splinted and control rabbits, for strain and thickness.

Biochemical and Histological Analysis of the TMJ Fibrocartilage

For biochemical analysis, TMJ disc and condylar fibrocartilage samples were prepared from the same samples used in compression testing including the 2 mm punches of the disc and the fibrocartilage that was cut and scraped off of the condyles ($n=8$). Samples were prepared for digestion by first hydrating in PBS for at least one hour, and then the samples were placed in individual tubes and the wet weights were recorded. A speed vacuum was used to dry the samples over night, and then the dry weights of the samples were recorded. Samples were then digested in 1 mL of a 125 $\mu\text{g/mL}$ papain solution over night at 60 °C (32). All biochemical assays were performed on aliquots from the same digest. The total collagen content of the TMJ fibrocartilages was determined using a well-established hydroxyproline assay (33). The content of glycosaminoglycan (GAG) was detected with the Sulfated Glycosaminoglycan Assay kit (Blyscan, Northern Ireland). The DNA content of the digest

was measured using a PicoGreen dsDNA Kit (Molecular Probes, Inc., Eugene, Oregon). A two-way ANOVA was completed with Tukey's post hoc test ($p < 0.05$) to determine for each biochemical assay, if there were differences between left and right sides and splinted and control rabbits for the TMJ disc and condylar fibrocartilage individually.

For histology, condyle samples from control and splinted rabbits ($n=3$) were fixed and decalcified in Formical (Decal Chemical Corp) to prepare for standard paraffin embedding and sectioning. Samples were embedded and sectioned by Alizeé Pathology (Thurmont, MD) at $6 \mu\text{m}$. Slides from the condylar fibrocartilage were stained with Hematoxylin and Eosin (H&E) to visualize the cells, Safranin O (SafO) for GAG, and a for Collagen Type II (Col II) immunostain (34).

Results

TMJ Disc

Under unconfined compression stress relaxation, there were no statistically significant differences between the left and right TMJ discs, nor between discs from splinted and control rabbits for any variable at any strain level (Figure 4A, B, C). With all sample types the maximum stress and tangent modulus increased with each strain step (Figure 4A, B). At 10% the average stress for all discs was 29 ± 12 kPa, at 15% it was 51 ± 20 kPa, at 20% it was 87 ± 32 kPa, at 25% it was 144 ± 48 kPa, and at 30% it was 225 ± 67 kPa. The average tangent modulus for all samples was 440 ± 235 kPa, 812 ± 354 kPa, 1412 ± 577 kPa, 2228 ± 767 kPa, and 3332 ± 931 kPa for each strain step 10-30%. The percent relaxation remained fairly constant across groups and strain points at approximately 65% (Figure 4C).

There were also no statistically significant biochemical differences between left and right TMJ disc or discs from splinted and control rabbits. The overall average of the disc samples were approximately $67.3 \pm 4.4\%$ water by weight (Figure 5A). For the disc, the overall average of the total collagen content was approximately $70.1 \pm 8.6\%$ dry weight (Figure 5B). The overall average of the GAG content of the discs was approximately $1.78 \pm 0.55\%$ dry weight (Figure 5C). The overall average of the DNA content was approximately $0.11 \pm 0.02\%$ dry weight (Figure 5D). No histological differences were observed (data not shown).

Condylar Fibrocartilage

For the mechanical testing, there were no statistical differences between the left and right condyles, however the strain at 0.02 N of the posterior region of the normal condyles was significantly higher than the strain of the treated condyles (splinted 0.37 ± 0.13 mm/mm, control 0.25 ± 0.06 mm/mm, $p < 0.05$, Figure 6A). The overall average posterior thickness was 0.20 ± 0.09 mm and the anterior thickness was 0.08 ± 0.03 mm (Figure 6B).

The biochemical results for the condylar fibrocartilage were fairly consistent between all samples left and right, as well as between splinted and control samples. The overall average of the condyle samples was approximately $73.2 \pm 4.4\%$ water by weight (Figure 5A). The overall average of total collagen content was approximately $67.1 \pm 12.7\%$ dry weight for all samples (Figure 5B), and the GAG content was approximately $1.78 \pm 0.70\%$ dry weight for

all of the condyles (Figure 5C). The only statistically significant difference between the control and the splinted condyles was for DNA content (Figure 5D). The control condyles were $0.29 \pm 0.05\%$ dry weight DNA while the splinted condyles were $0.20 \pm 0.09\%$ dry weight DNA ($p < 0.05$).

Histological analysis revealed an almost complete loss of the subchondral layer of the fibrocartilage, in the posterior regions of the contralateral splinted rabbit condyles. This loss was accompanied by a loss of defined cell layers, and only a fibrous layer remaining to cover the bone. This change is illustrated with whole condyles stained with H&E, Safo, and Col II immunostain (Figure 7, 4X magnification), where differences in anterior (Figure 8, 10X magnification) and posterior (Figure 9, 10X magnification) regions of the condyles, respectively, can be seen for all stain types. On the H&E stained slides, the lacunae appear to be losing their shape and columnar nature and the subchondral region of the fibrocartilage were seen to shrink in both of the splinted condyles (Figures 7- 9; parts C and D) compared to the control condyles (Figures 7- 9; parts A and B). GAG staining revealed a change in distribution between the controls (Figures 7- 9; parts E and F) and the splinted condyles (Figures 7- 9; parts G and H). GAG staining was seen throughout the length of the treated condyle and the normal condyles. However, GAG stained regions seem to be thinner in the contralateral splinted condyles compared to the normal condyles. A similar pattern of changes as the GAG was seen in the Col II staining for the splinted condyles (Figures 7- 9; parts K and L) as compared to the control (Figures 7- 9; parts I and J) condyles. A difference was also noted between the treated and contralateral sides of the splinted rabbits. For both the GAG and Col II staining in the contralateral condyle, the GAG and Col II layer ended approximately midway through the anterior-posterior length of the condyle. The GAG and Col II staining was in the anterior regions (Figure 8 G and K) but not the posterior regions (Figure 9 G and K).

Discussion

The primary observation from this study was that unilateral splint placement can drive uneven condylar fibrocartilage degeneration, as measured mechanically, biochemically, and as seen in histology. The uneven effect of the splint, between the treated and contralateral sides was more pronounced in the posterior region of the condyle. Overall, splint placement resulted in the degeneration of the subchondral collagen type II/GAG rich layer of the contralateral condylar fibrocartilage, while having little effect on the TMJ disc. Furthermore, it was shown that condylar fibrocartilage degeneration can occur with the TMJ disc in its correct anatomical location (no displacement). No changes were found in the mechanical properties of the TMJ disc, which agreed with the lack of changes in the biochemistry and histology of the disc. The TMJ disc properties generally agreed with previous studies of the normal TMJ disc in both the mechanical behavior and the biochemical composition (28, 35). These results support a shift in focus from the TMJ disc to the condylar fibrocartilage in terms of the initial sources of TMJ pain and degeneration.

In terms of the condyle, the rabbit unilateral splint model seemed to affect the deep subchondral cartilage layer more than the surface fibrous layer. The histology agreed with a previous rabbit molar splint study where the splinting seemed to affect the deep cartilage

layer (13). A connection between the compressive properties of TMJ fibrocartilage after 6 weeks of splinting and the changes in histology was observed. The condylar fibrocartilage compressive data suggested that abnormal loading causes changes in the extracellular matrix distribution of TMJ fibrocartilage leading to stiffer fibrocartilage. The posterior region of the splinted condyles was stiffer than the control tissue, for the same force/stress there was less displacement. In terms of the boundary conditions for indentation, the indenter was much smaller than the condyle surface. However, the distance travelled by the indenter was much less than the diameter, which is a limitation of the approach. In the future, a smaller indenter will be used (~200 micrometers), with a curved tip and porous.

The changes were not yet apparent in the biochemistry of the condylar fibrocartilage except in the DNA content; which could correspond to the changes with the loss of the cell layers of the cartilage layer seen in histology. Lack of change measured in GAG content could be attributed to isolation of the thin fibrocartilage for digestion. A regional isolation, anterior and posterior, was not possible, which would likely show a decrease in GAG content in the posterior of the contralateral condylar fibrocartilage. One possible way to capture more of the GAG content regionally would be to digest the fibrocartilage on the bone, to prevent leaving a layer of the fibrocartilage on the bone after scraping the fibrocartilage off of the bone for the digest.

The unilateral splint model was advantageous because the joint capsule was not penetrated. This particular splint model will allow future studies to focus on removing the splints at various time points to gain a better understanding of how/when degeneration becomes an irreversible condition. This rabbit model will also allow for a multidisciplinary approach to understanding TMDs by allowing other analyses such as pain and kinematic assessments to be incorporated. This TMD animal model also had limitations. While the rabbit is larger than many TMD animal models, it still only provided a limited amount of soft tissue for testing. The rabbit mouth was also small and was difficult to access for dental procedures. This model also did not drive changes to the TMJ disc at 6 weeks.

We do believe this rabbit splint model is worth pursuing because it provides a mechanical mechanism for degeneration of the TMJ articulating tissues (3). We have shown that abnormal loading leads to stiffer condylar fibrocartilage. Other mechanical properties can also be affected, such as shear (36, 37) and friction (3, 38). The increased friction could displace the disc, leading to further degeneration. As such, more modes of mechanical testing are needed, and at longer time points, to test these hypotheses, that only larger animal models allow.

The results of this study suggest a possible explanation as to why some patients have TMJ pain, but no TMJ disc problems. With this particular model, the TMJ condyle was undergoing changes, while no changes were observed in the TMJ disc. Thus, it is possible that there is condylar fibrocartilage degeneration in some TMD patients which cannot be detected with current imaging techniques. Importantly, degeneration of the condylar fibrocartilage may be the source of mediators responsible for their pain. This research raises the question whether disc derangement is necessary for TMJ osteoarthritis to occur, or whether mild osteoarthritis is enough to cause pain. Longer time points are necessary to

determine if disc degeneration would start to occur. While more studies are needed to understand the link between TMJ degeneration and the development of TMJ pain, if degeneration of the fibrocartilage is the trigger for pain, it will be essential to determine whether these changes are reversible following normalization of joint loading, as it is conceivable that in chronic TMD patients, the degeneration has reached a point at which it is no longer reversible.

TMD is very complex and a disease that has a progression that is multifactorial. There are many types of assessments that can be used to study TMD degeneration and pain. This study only assessed one potential mechanism, altered occlusion, which could lead to osteoarthritis. This one particular altered occlusion model has many aspects that can be analyzed. We hypothesize that the splint caused the vertical space to increase in the ipsilateral joint and decrease in the contralateral joint, which would alter the loading in both sides. There were trends that the contralateral side had more distinct remodeling than the ipsilateral side. It is interesting that condylar remodeling was observed with no changes in the disc with the parameters tested. Perhaps the changes would show up with other testing modalities, such as shear or friction testing. It will also be important to take the study out to longer time points to see if the disc remains 'normal' or if it begins to have observable remodeling as well. Often times in the clinic disc displacement and condylar degeneration go hand in hand, but in other cases TMD patients can have pain but no imaged abnormalities. Perhaps this altered occlusion model captures this phenomenon. In a pain assessment study with the same altered occlusion model, the pain response of the rabbits was increased from the altered occlusion at six weeks (39). The changes to the condylar cartilage described here would not be able to be picked up on standard imaging technology, perhaps elucidating why some patients report to the clinic with pain but no obvious imaged abnormalities.

Acknowledgments

We would like to acknowledge funding from the National Science Foundation under grant number 0812348, as well as from the National Institutes of Health under grant number T32 EB003392-01, the University of Pittsburgh Research Fund, and the University of Pittsburgh School of Dental Medicine.

References

1. Dym H, Israel H. Diagnosis and Treatment of Temporomandibular Disorders. *Dental Clinics of North America*. 2012; 56(1):149–161. [PubMed: 22117948]
2. Goldstein BH. Temporomandibular disorders: A review of current understanding. *Oral Surgery, Oral Medicine, Oral Pathology, Oral Radiology, and Endodontology*. 1999; 88(4):379–385.
3. Tanaka E, Detamore MS, Mercuri LG. Degenerative disorders of the Temporomandibular joint: etiology, diagnosis, and treatment. *Journal of Dental Research*. 2008; 87(4):296–307. [PubMed: 18362309]
4. Ingawalé S, Goswami T. Temporomandibular joint: Disorders, treatments, and biomechanics. *Annals of Biomedical Engineering*. 2009; 37(5):976–996. [PubMed: 19252985]
5. Zarb GA, Carlsson GE. Temporomandibular Disorders: Osteoarthritis. *Journal of Orofacial Pain*. 1999; 13(4):295–306. [PubMed: 10823044]
6. Cholasueksa P, Warita H, Soma K. Alterations of the rat temporomandibular joint in functional posterior displacement of the mandible. *Angle Orthodontist*. 2004; 74(5):677–683. [PubMed: 15529504]

7. Fuentes MA, Opperman LA, Buschang P, Bellinger LL, Carlson DS, Hinton RJ. Lateral functional shift of the mandible: Part I. Effects on condylar cartilage thickness and proliferation. *American Journal of Orthodontics and Dentofacial Orthopedics*. 2003; 123(2):153–159. [PubMed: 12594421]
8. Liu C, Kaneko S, Soma K. Glenoid fossa responses to mandibular lateral shift in growing rats. *Angle Orthodontist*. 2007; 77(4):660–667. [PubMed: 17605490]
9. Nakano H, Maki K, Shibasaki Y, Miller AJ. Three-dimensional changes in the condyle during development of an asymmetrical mandible in a rat: A microcomputed tomography study. *American Journal of Orthodontics and Dentofacial Orthopedics*. 2004; 126(4):410–420. [PubMed: 15470344]
10. Sato C, Muramoto T, Soma K. Functional lateral deviation of the mandible and its positional recovery on the rat condylar cartilage during the growth period. *Angle Orthodontist*. 2006; 76(4):591–597. [PubMed: 16808564]
11. Watanabe A, Yamaguchi M, Utsunomiya T, Yamamoto H, Kasai K. Histopathological changes in collagen and matrix metalloproteinase levels in articular condyle of experimental model rats with jaw deformity. *Orthodontics and Craniofacial Research*. 2008; 11(2):105–118. [PubMed: 18416752]
12. Wattanachai T, Yonemitsu I, Kaneko S, Soma K. Functional lateral shift of the mandible effects on the expression of eCM in rat temporomandibular cartilage. *Angle Orthodontist*. 2009; 79(4):652–659. [PubMed: 19537875]
13. Chaves K, Munerato MC, Ligocki A, Lauxen I, De Quadros OF. Microscopic Analysis of the Temporomandibular Joint in Rabbits (*Oryctolagus cuniculus* L.). Using An Occlusal Interference Cranio. 2002; 20(2):116–124.
14. Mao JJ, Rahemtulla F, Scott PG. Proteoglycan expression in the rat temporomandibular joint in response to unilateral bite raise. *Journal of Dental Research*. 1998; 77(7):1520–1528. [PubMed: 9663437]
15. Matsuka Y, Kitada Y, Mitoh Y, Adachi A, Yamashita A. Effects of a bite-raising splint on the duration of the chewing cycle and the EMG activities of masticatory muscles during chewing in freely moving rabbits. *Journal of Oral Rehabilitation*. 1998; 25(2):159–165. [PubMed: 9576602]
16. Proff P, Gedrange T, Franke R, Schubert H, Fanghanel J, Miede B, et al. Histological and histomorphometric investigation of the condylar cartilage of juvenile pigs after anterior mandibular displacement. *Annals of Anatomy*. 2007; 189(3):269–275. [PubMed: 17534034]
17. Serogl HG, Farmand M. Experiments with unilateral bite planes in rabbits. *Angle Orthodontist*. 1975; 45(2):108–114. [PubMed: 1054937]
18. Shaw RM, Molyneux GS. The effects of induced dental malocclusion on the fibrocartilage disc of the adult rabbit temporomandibular joint. *Archives of Oral Biology*. 1993; 38(5):415–422. [PubMed: 8328922]
19. Sindelar BJ, Evanko SP, Alonzo T, Herring SW, Wight T. Effects of intraoral splint wear on proteoglycans in the temporomandibular joint disc. *Arch Biochem Biophys*. 2000; 379(1):64–70. [PubMed: 10864442]
20. Almarza AJ, Hagandora CK, Henderson SE. Animal models of temporomandibular joint disorders: Implications for tissue engineering approaches. *Annals of Biomedical Engineering*. 2011; 39(10):2479–2490. [PubMed: 21822741]
21. Ali AM, Sharawy MM. Alteration in fibronectin of the rabbit craniomandibular joint tissues following surgical induction of anterior disk displacement: Immunohistochemical study. *Acta Anatomica*. 1995; 152(1):49–55. [PubMed: 7604678]
22. Axelsson S, Holmlund A, Hjerpe A. An experimental model of osteoarthritis in the temporomandibular joint of the rabbit. *Acta Odontologica Scandinavica*. 1992; 50(5):273–280. [PubMed: 1441931]
23. Timmis DP, Aragon SB, Van Sickels JE, Aufdemorte TB. Comparative study of alloplastic materials for temporomandibular joint disc replacement in rabbits. *Journal of Oral and Maxillofacial Surgery*. 1986; 44(7):541–554. [PubMed: 3522828]
24. Tominaga K, Alstergren P, Kurita H, Kopp S. Serotonin in an antigen-induced arthritis of the rabbit temporomandibular joint. *Archives of Oral Biology*. 1999; 44(7):595–601. [PubMed: 10414874]

25. Tominaga K, Yamada Y, Fukuda J. Changes in chewing pattern after surgically induced disc displacement in the rabbit temporomandibular joint. *Journal of Oral and Maxillofacial Surgery*. 2000; 58(4):400–405. [PubMed: 10759120]
26. Ueki K, Takazakura D, Marukawa K, Shimada M, Nakagawa K, Takatsuka S, et al. The use of polylactic acid/polyglycolic acid copolymer and gelatin sponge complex containing human recombinant bone morphogenetic protein-2 following condylectomy in rabbits. *Journal of Cranio-Maxillofacial Surgery*. 2003; 31(2):107–114. [PubMed: 12628601]
27. Allen KD, Athanasiou KA. A surface-regional and freeze-thaw characterization of the porcine temporomandibular joint disc. *Annals of Biomedical Engineering*. 2005; 33(7):951–962. [PubMed: 16060536]
28. Hagandora CK, Chase TW, Almarza AJ. A Comparison of the Mechanical Properties of the Goat Temporomandibular Joint Disc to the Mandibular Condylar Cartilage in Unconfined Compression. *Journal of Dental Biomechanics*. 2011; 2(1)
29. Cohen B, Lai WM, Mow VC. A transversely isotropic biphasic model for unconfined compression of growth plate and chondroepiphysis. *Journal of Biomechanical Engineering*. 1998; 120(4):491–496. [PubMed: 10412420]
30. Sergerie K, Lacoursière MO, Lévesque M, Villemure I. Mechanical properties of the porcine growth plate and its three zones from unconfined compression tests. *Journal of Biomechanics*. 2009; 42(4):510–516. [PubMed: 19185303]
31. Swann AC, Seedhom BB. Improved techniques for measuring the indentation and thickness of articular cartilage. *Proceedings of the Institution of Mechanical Engineers, Part H: Journal of Engineering in Medicine*. 1989; 203(3):143–150.
32. Farndale RW, Sayers CA, Barrett AJ. A direct spectrophotometric microassay for sulfated glycosaminoglycans in cartilage cultures. *Connect Tissue Res*. 1982; 9(4):247–248. [PubMed: 6215207]
33. Almarza AJ, Bean AC, Baggett LS, Athanasiou KA. Biochemical analysis of the porcine temporomandibular joint disc. *British Journal of Oral and Maxillofacial Surgery*. 2006; 44(2):124–128. [PubMed: 16011866]
34. Detamore MS, Orfanos JG, Almarza AJ, French MM, Wong ME, Athanasiou KA. Quantitative analysis and comparative regional investigation of the extracellular matrix of the porcine temporomandibular joint disc. *Matrix Biol*. 2005; 24(1):45–57. [PubMed: 15749001]
35. Kalpakci KN, Willard VP, Wong ME, Athanasiou KA. An interspecies comparison of the temporomandibular joint disc. *Journal of Dental Research*. 2011; 90(2):193–198. [PubMed: 21118792]
36. Tanaka E, Iwabuchi Y, Rego EB, Koolstra JH, Yamano E, Hasegawa T, et al. Dynamic shear behavior of mandibular condylar cartilage is dependent on testing direction. *Journal of Biomechanics*. 2008; 41(5):1119–1123. [PubMed: 18242620]
37. Tanaka E, Rego EB, Iwabuchi Y, Inubushi T, Koolstra JH, Van Eijden TMGJ, et al. Biomechanical response of condylar cartilage-on-bone to dynamic shear. *Journal of Biomedical Materials Research - Part A*. 2008; 85(1):127–132. [PubMed: 17688244]
38. Tanaka E, Iwabe T, Dalla-Bona DA, Kawai N, Van Eijden T, Tanaka M, et al. The effect of experimental cartilage damage and impairment and restoration of synovial lubrication on friction in the temporomandibular joint. *Journal of Orofacial Pain*. 2005; 19(4):331–336. [PubMed: 16279485]
39. Henderson SE, Tudares MA, Gold MS, Almarza AJ. Analysis of Pain in the Rabbit Temporomandibular Joint after Unilateral Splint Placement. *Journal of Oral and Facial Pain and Headache*. 2014 Accepted.

Highlights

Splinted rabbit condylar fibrocartilage was significantly stiffer than control.

Splinted rabbit condylar fibrocartilage had significantly less DNA content.

Loss of condylar fibrocartilage layers observed in histology.

The change in joint loading led to condylar damage without observable disc damage.

Unilateral splint placement can drive uneven condylar fibrocartilage degeneration.

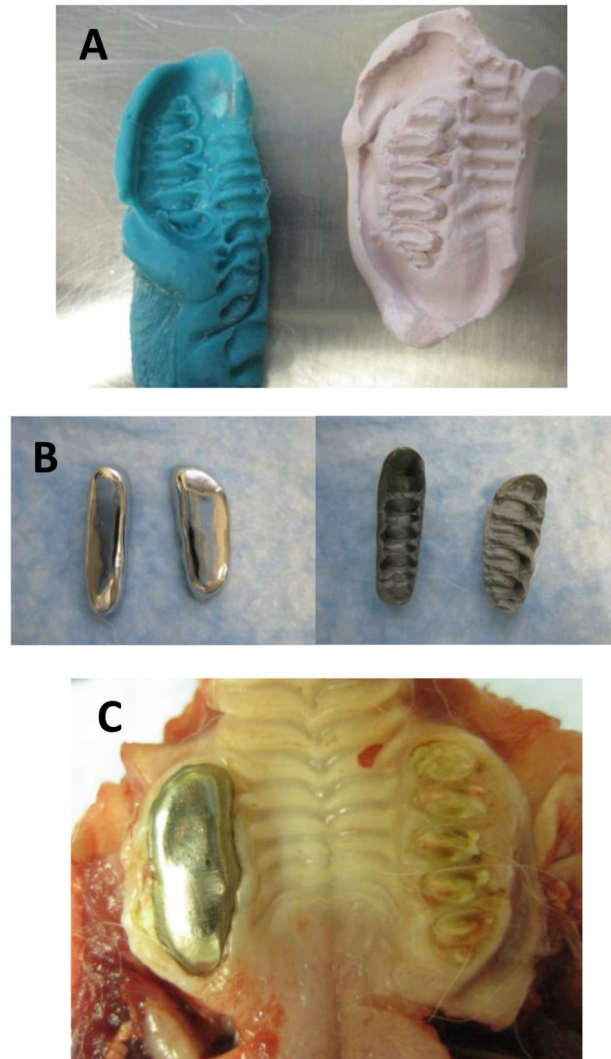


Figure 1. Unilateral molar bite raising splints. A) The splints were made by first taking an impression of the teeth, from which a plaster mold was made. B) The metal splints were cast as crowns, the superior and inferior views are shown. C) Upper splint in place after 6 weeks.

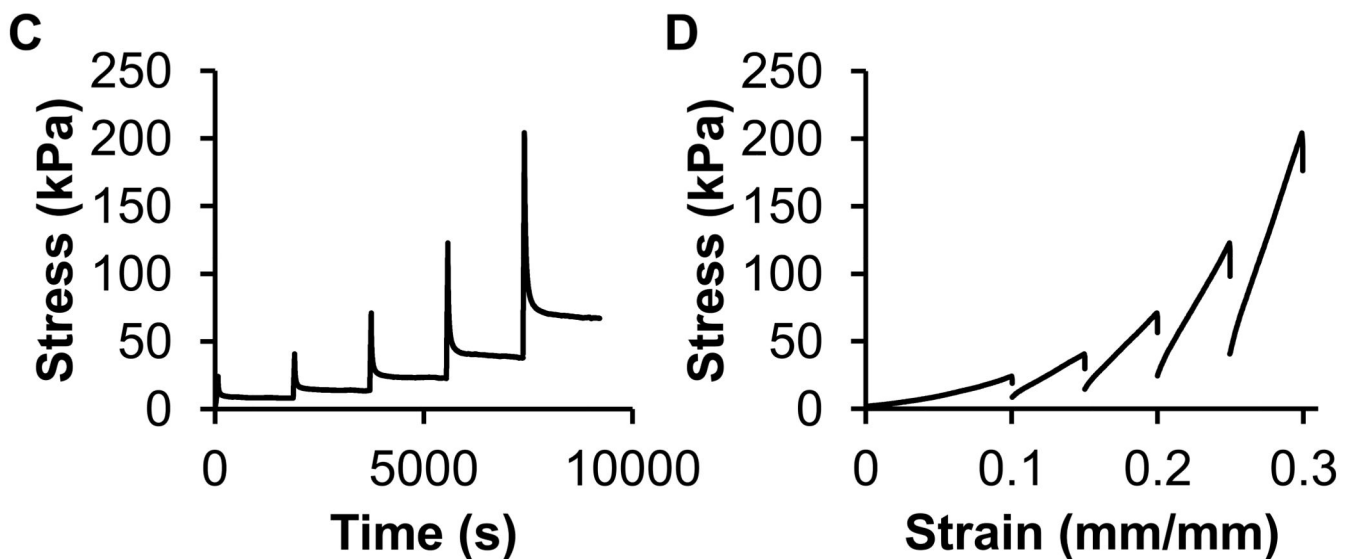
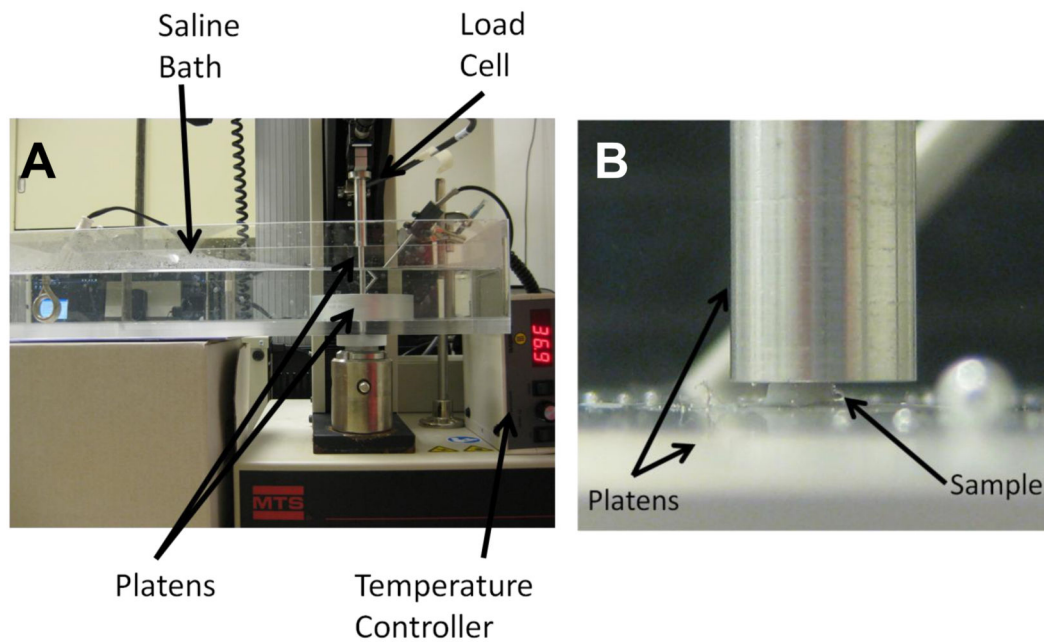


Figure 2.

Unconfined compression of the TMJ disc. A) Unconfined compression testing set up. Samples were tested in a saline bath at 37 °C. B) Picture shows a representative TMJ disc sample and the platens. C) Stress of the TMJ disc sample over time. Each strain step is shown consecutively. Samples were compressed to the strain level (10%, 15%, 20%, 25%, 30%) and allowed to relax for 30 minutes. Representative curves are shown. D) Stress-strain loading curves for the TMJ disc. Representative curves are shown for each strain step 10%-30% with 5% increments.

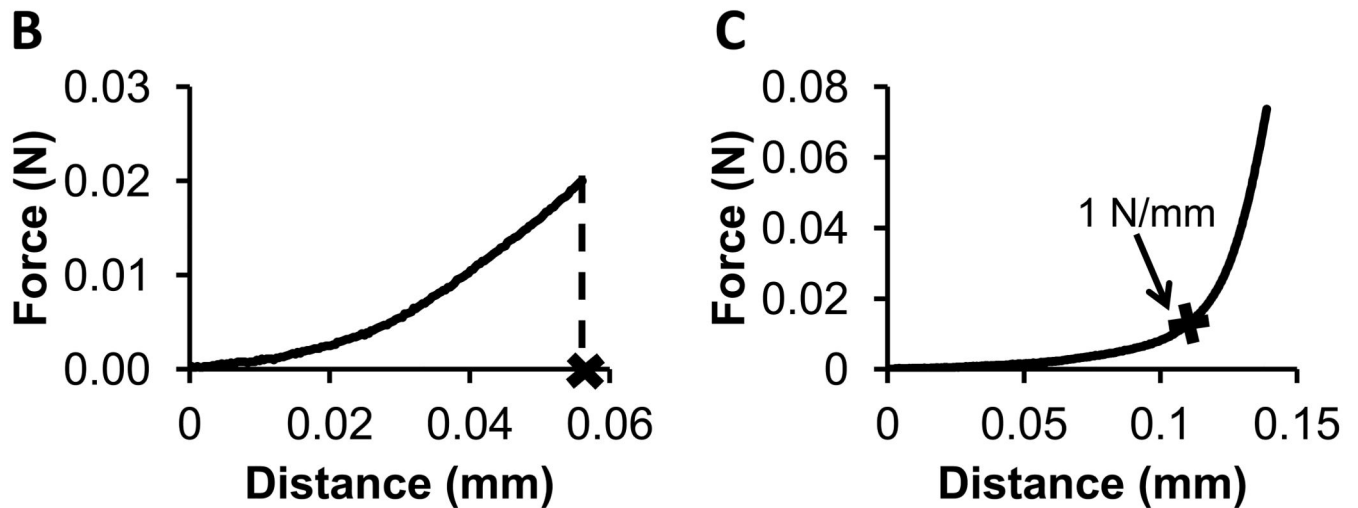
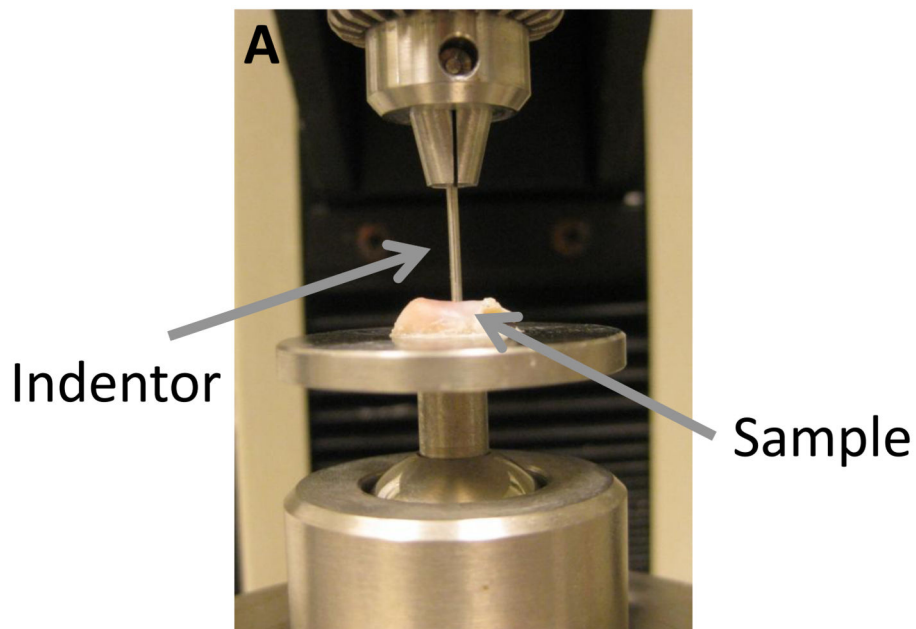


Figure 3. Compression testing to a particular force. A) Whole condyles were glued to a rotating stage allowing for multiple testing locations. The indenter was 1 mm in diameter. Samples were kept hydrated with PBS between testing steps. B&C) Condylar fibrocartilage loading curves. B) Representative loading curve to 0.02 N for compression testing of the condylar fibrocartilage, where the distance is used as displacement for strain. C) Representative loading curve for the thickness test of the condylar fibrocartilage. The thickness was the distance in the region where the slope rapidly changed, at the point where the slope was equal to 1 N/mm.

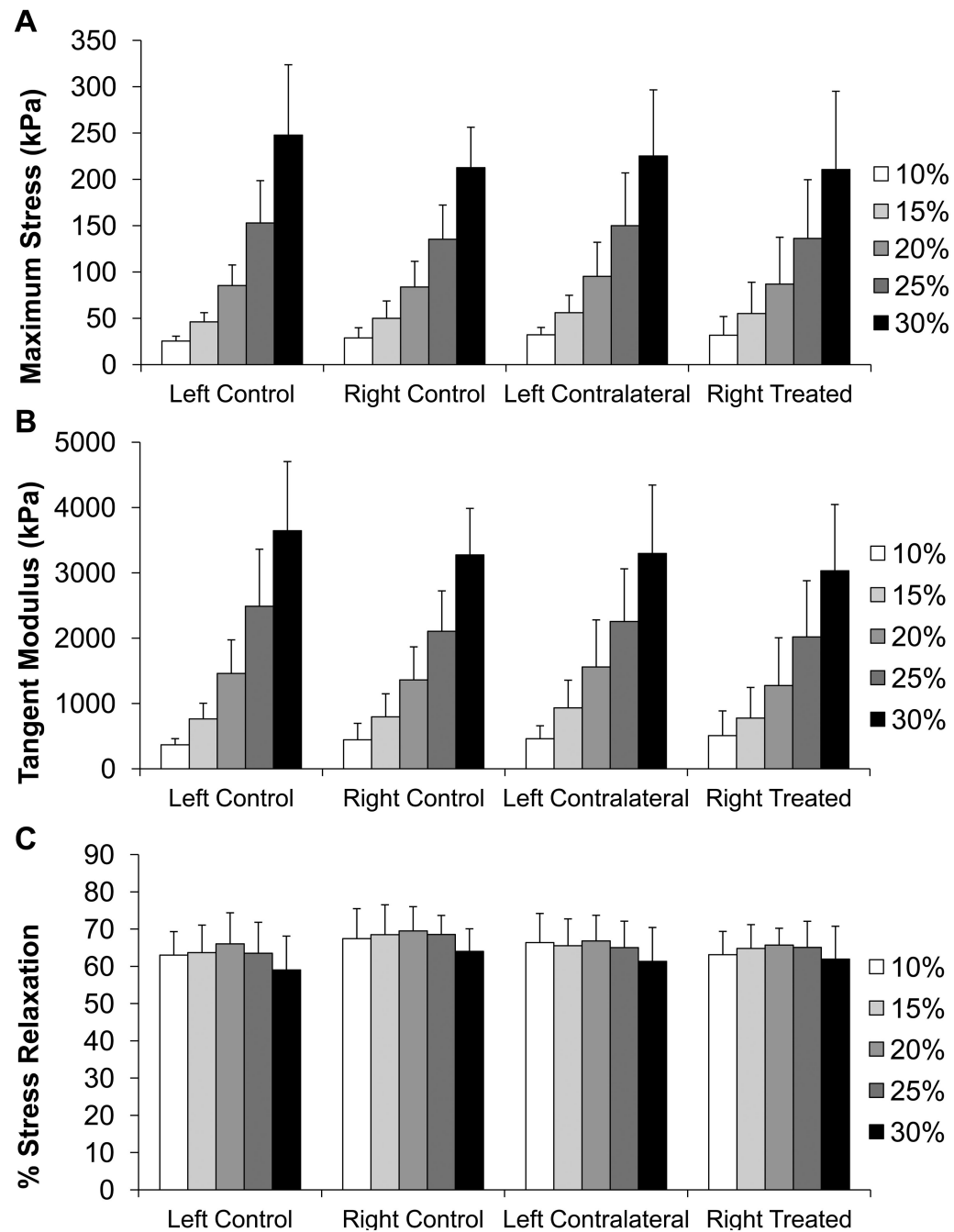


Figure 4.

TMJ disc unconfined compression results. A) Maximum stress for each strain step of unconfined compression for each TMJ disc tested. No statistical differences were seen between groups at any strain level. B) Tangent modulus for each strain step in unconfined compression for each TMJ disc tested. No statistical differences were seen between groups at any strain level. C) Percent stress relaxation for each strain step in unconfined compression for each TMJ disc tested. No statistical differences were seen between groups at any strain level. Sample size of n=8 per group. All error bars are standard deviations.

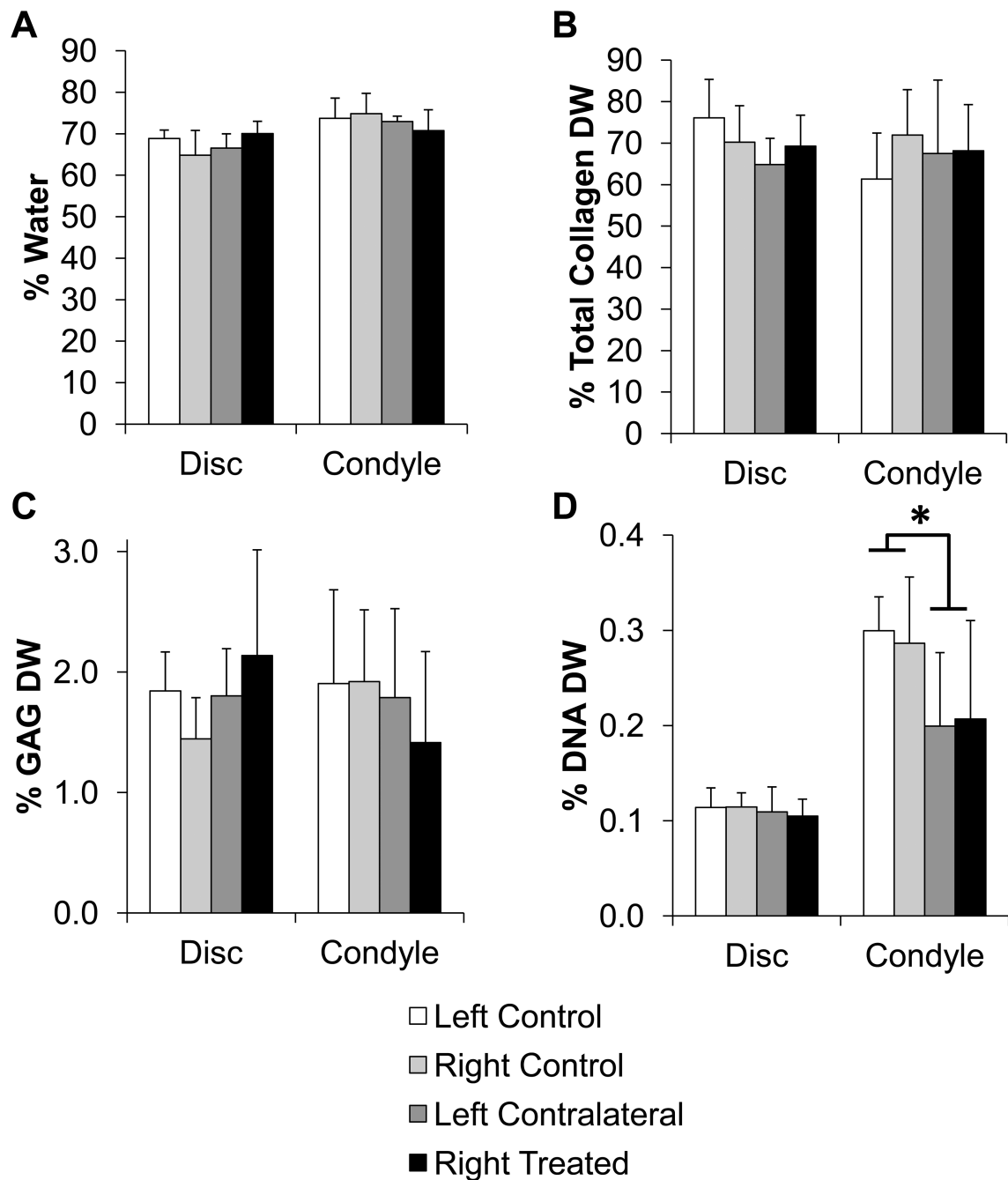


Figure 5. Biochemical composition for the TMJ disc and condylar fibrocartilage. A) Water content, B) Total collagen content per dry weight, C) GAG content per dry weight, D) DNA content per dry weight. The only statistical difference was in the condylar fibrocartilage DNA content with the average of the splinted condyles being less than the average of the control condyles ($p < 0.05$). Sample size of $n=8$ per group. Data shown as average \pm standard deviation.

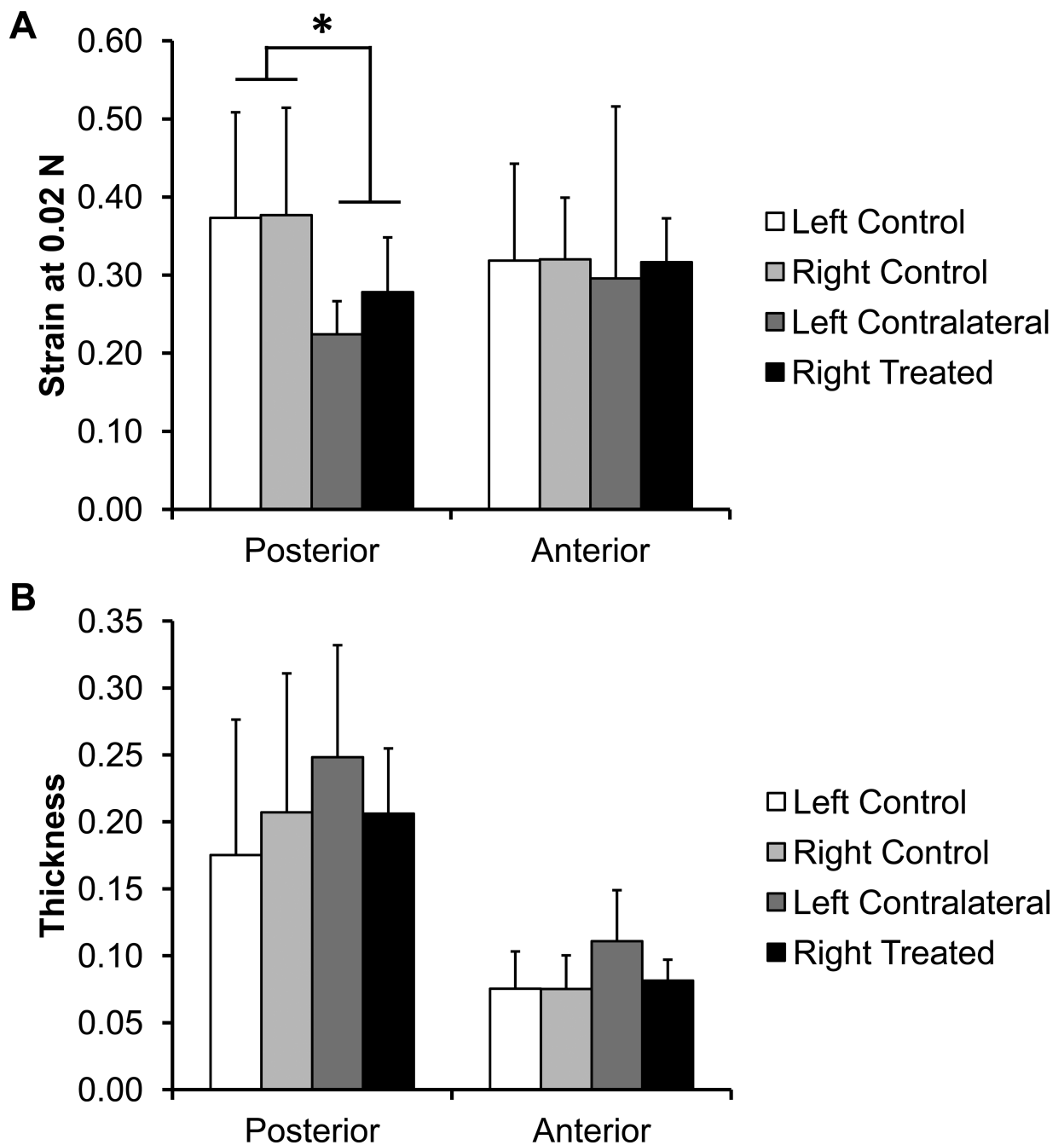


Figure 6. Condylar fibrocartilage compression results. A) Strain of the condylar fibrocartilage at 0.02 N of loading, as compression testing to a particular force was used on the TMJ condyles regionally. The posterior region of the splinted rabbit condyles was significantly stiffer than the control fibrocartilage. (* $p < 0.05$) No other statistically significant differences were observed. B) Thickness of the TMJ condylar fibrocartilage. No statistically significant differences were observed. Sample size of $n=8$ per group. All error bars are standard deviations.

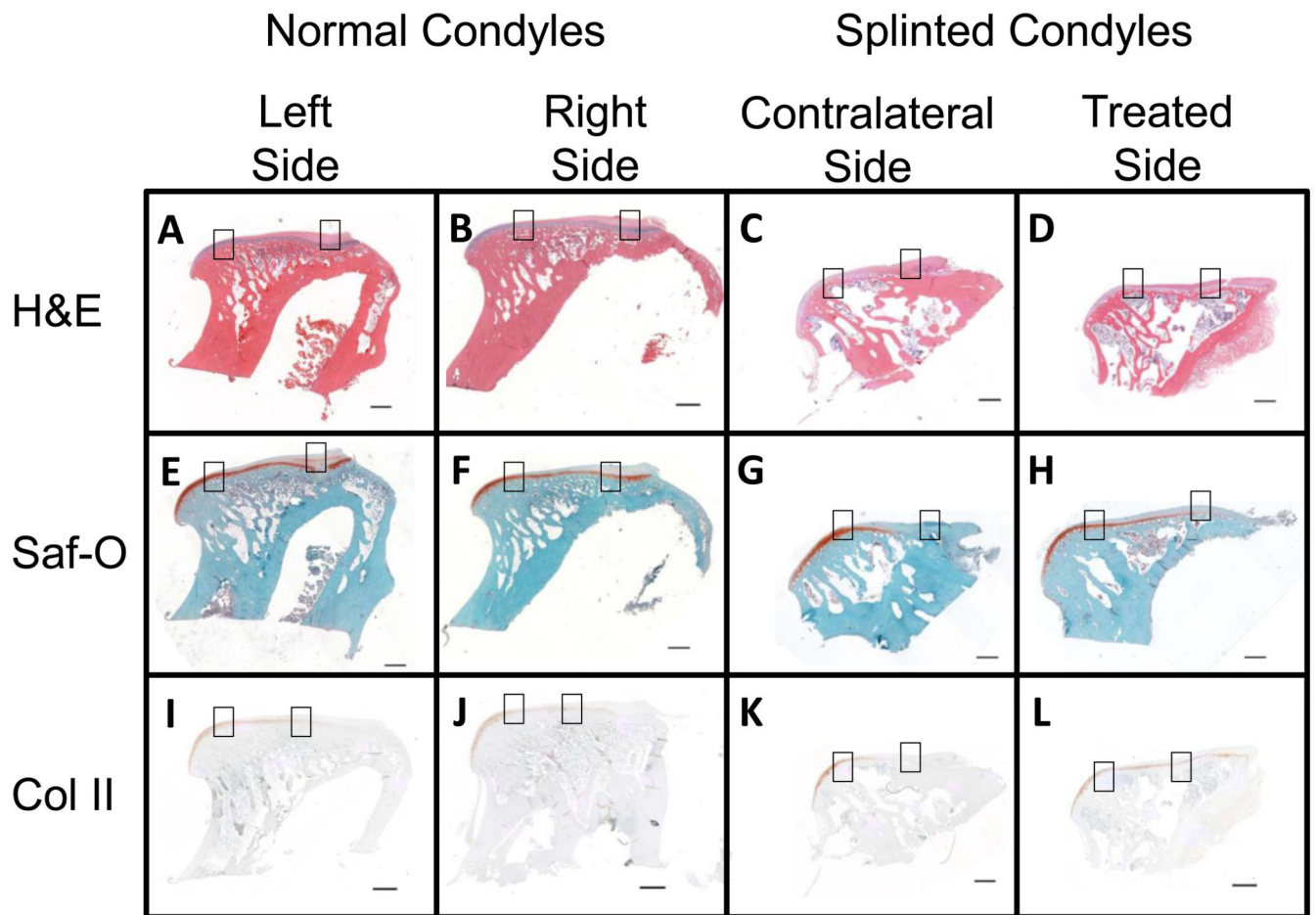


Figure 7.

Histology showing the entire condyles at 4X magnification (scale bars = 1 mm). Boxes indicate the areas shown in Figures 8 and 9 at 10X magnification. Figure 8 shows the anterior regions (boxes on the left of the images). Figure 9 shows the posterior regions (boxes on the right of the images). Staining used for comparison included H&E, Saf-O for GAG staining, and Collagen Type 2 immunostain. The right and left condyles of control animals were compared to the left (contralateral) and right (treated) condyles of splinted animals. Representative pictures shown from at least n=3.

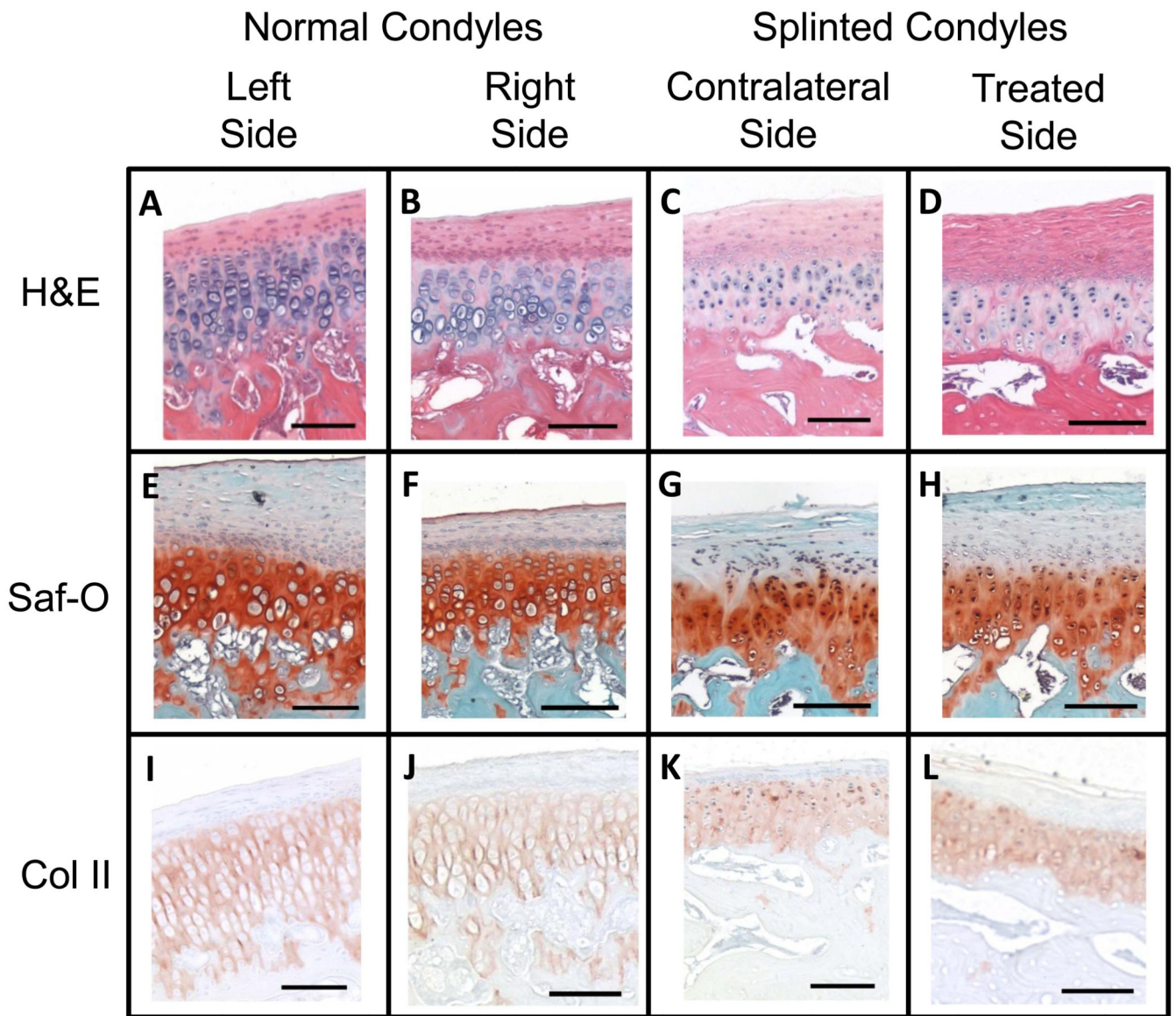


Figure 8.

Histology showing the anterior regions of the TMJ condyles at 10X magnification (scale bars = 100 μ m). Boxes showing the location of each image were in Figure 7 on the left of each figure. Staining used for comparison included H&E, Saf-O for GAG staining, and Collagen Type 2 immunostain. The right and left condyles of control animals were compared to the left (contralateral) and right (treated) condyles of splinted animals. Representative pictures shown from at least n=3.

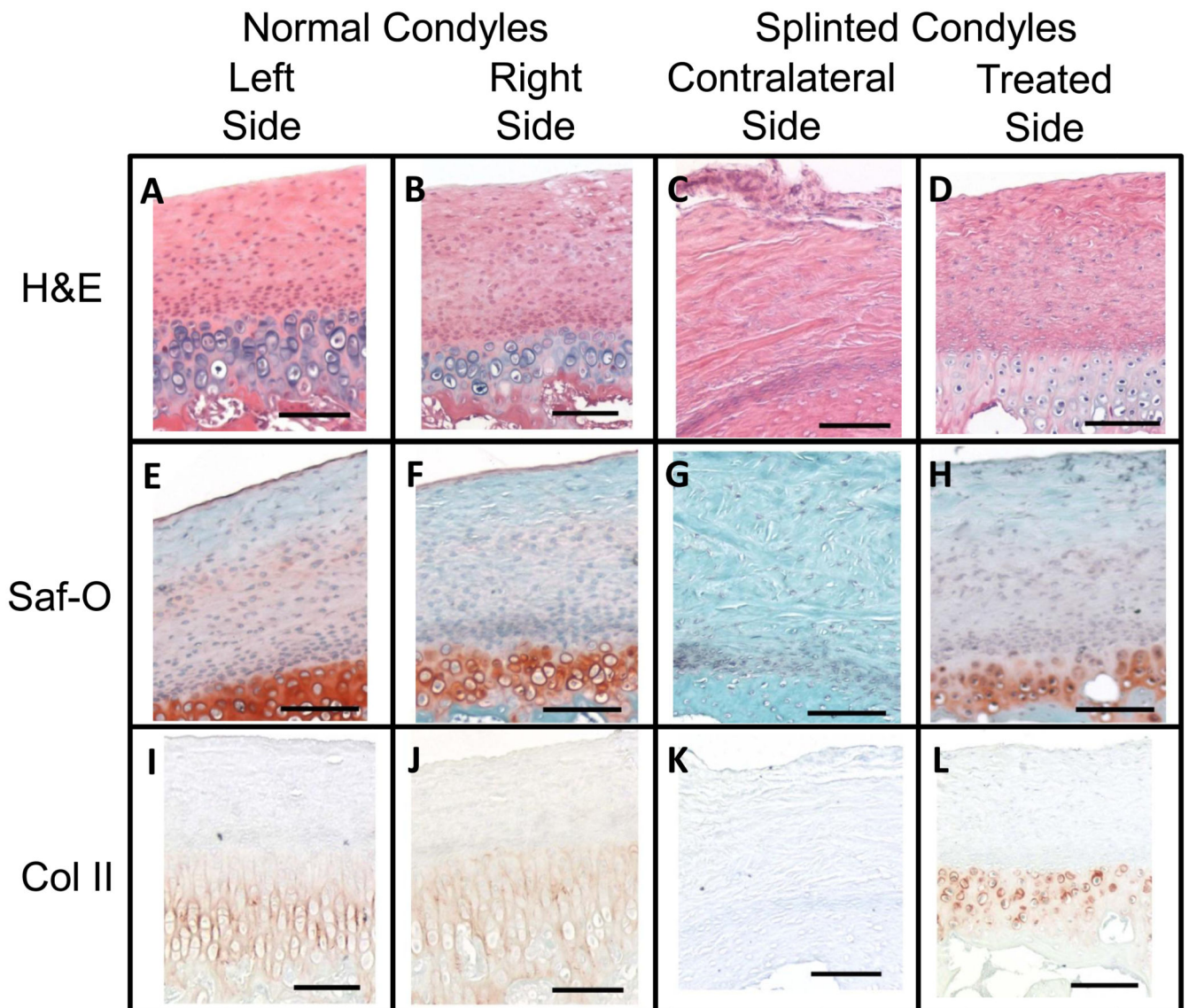


Figure 9.

Histology showing the posterior regions of the TMJ condyles at 10X magnification (scale bars = 100 μ m). Boxes showing the location of each image were in Figure 7 on the right of each image. Staining used for comparison included H&E, Saf-O for GAG staining, and Collagen Type 2 immunostain. The right and left condyles of control animals were compared to the left (contralateral) and right (treated) condyles of splinted animals. Representative pictures shown from at least n=3.